Planta (2025) 261:20
https://doi.org/10.1007/s00425-024-04597-7

SHORT COMMUNICATION

Agropine-type *rolA* modulates ROS homeostasis in an auxin-dependent manner in *rolA*-expressing cell cultures of *Rubia cordifolia* L.

Galina N. Veremeichik[1] · Taisia O. Solomatina[1] · Anastasia A. Khopta[1] · Evgenia V. Brodovskaya[1] · Tatiana Yu. Gorpenchenko[1] · Valeria P. Grigorchuk[1] · Dmitrii V. Bulgakov[1] · Victor P. Bulgakov[1]

Received: 20 October 2024 / Accepted: 17 December 2024

Abstract

Main conclusion **Long-term cultured calli may experience a biosynthetic shift due to the IAA-dependent expression of the rolA gene, which also affects ROS metabolism.**

Abstract The "hairy root" syndrome is caused by the root-inducing Ri-plasmid of *Rhizobium rhizogenes,* also known as *Agrobacterium rhizogenes*. The Ri-plasmid contains genes known as *rol* genes or root oncogenic loci, which promote root development. The important implications of the *rolA* gene from the T-DNA include reduced plant size, resistance to infections, and the activation of specialised metabolism. Nevertheless, *rolA* does not belong to the *plast* gene group because its function is still uncertain. Recent investigations have shown two important effects of the *rolA* gene. First, the production of secondary metabolites has changed in long-term cultivated *rolA*-transgenic calli of *Rubia cordifolia* L. Second, the expression of both the *rolA* and *rolB* genes has a strong auxin-dependent antagonistic effect on reactive oxygen species (ROS) homeostasis. In this work, we attempted to elucidate two *rolA* gene phenomena: what caused the secondary metabolism of long-term cultured calli to change? How does the individual expression of the *rolA* gene affect ROS homeostasis? We analysed SNPs in the 5′ untranslated region and coding region of the *rolA* gene. These mutations do not affect the known essential amino acids of the RolA proteins. Notably, in the promoter of the *rolA* gene, an ACTTTA motif for auxin-mediated transcription factors was identified. Using two separate cell cultures, we demonstrated the strong auxin dependence of *rolA* gene expression. The expression of genes involved in ROS metabolism decreased in response to an auxin-mediated increase in *rolA* gene expression. Two assumptions can be made. The long-term cultivation of calli may cause changes in the hormonal state of the culture over time, which may modulate the action of the RolA protein. Moreover, auxin-dependent expression of the *rolA* gene led to a decrease in ROS metabolism. It can be assumed that the antagonistic interaction between *rolA* and *rolB* prevents strong *rolB*-induced auxin sensitivity and oxidative bursts to balance the cell state.

Keywords Anthraquinone · Auxins · Callus culture · *Rhizobium rhizogenes* · Reactive oxygen species · Hairy root" · *Rol*A oncogene

Abbreviations

AQ	Anthraquinones
PGR	Plant growth regulators
Rol	Root oncogenic locus
ROS	Reactive oxygen species
T-DNA	Transfer DNA
UTR	Untranslated region

Communicated by Dorothea Bartels.

✉ Galina N. Veremeichik
gala-vera@mail.ru

[1] Federal Scientific Center of the East Asia Terrestrial Biodiversity of the Russian Academy of Sciences Far Eastern Branch, FGBUN FNC Bioraznoobrazia Nazemnoj Bioty Vostocnoj Azii Dal'nevostocnogo Otdelenia Rossijskoj Akademii Nauk, Vladivostok 690022, Russia

Published online: 23 December 2024

Introduction

The biodiversity gained through horizontal gene transfer involves both prokaryotes and eukaryotes (Aubin et al. 2021). Extensive research on the transfer of genes from *Agrobacterium* to plants has revealed the possibility of a symbiotic relationship between plants and agrobacteria. The "hairy root" syndrome is caused by oncogenes from the transfer DNA (T-DNA) of the root-inducing Ri-plasmid of *Rhizobium rhizogenes* (also known as *Agrobacterium rhizogenes*). The T-DNA of the Ri-plasmid contains genes known as *rol* genes or root oncogene loci, which promote root development. A comprehensive examination of the effects of individual and joint expression of these genes has proven the biotechnological importance of *rol* genes as activators of the specialised metabolism of medicinal plants (Bulgakov et al. 2011; Vereshchagina et al. 2014; Sarkar et al. 2018). Furthermore, the stress resistance of transgenic plants is significantly regulated by *rol* genes (Guo et al. 2019; Gutierrez-Valdes et al. 2020; Pujari and Babu 2022; Veremeichik et al. 2022). *Rol* genes have been identified in the genomes of several plant species (Matveeva and Otten 2021; Chen et al. 2022). The significant benefits of *rol* gene expression on metabolism, the production of aberrant development, and the rerouting of roots and other plant organ growth have been shown for naturally occurring transformants (Desmet et al. 2021). Owing to the potential to use *rol* genes to improve the properties of crop and noncrop-cultured plants, Japan and a few other countries exempt wild-type Ri-plants from legal control of genetically modified organisms or GMOs (Desmet et al. 2020a; Smytch et al. 2021; Philips et al. 2022). Thus, determining the nature and function of the *rol* genes in *R. rhizogenes* is an important field of research.

Among the other *rol* genes, the function of the *rolA* gene is still the most unclear and poorly understood (Veremeichik et al. 2023a). The *rolA* gene is the 10th open reading frame (ORF) of the 18 ORFs of the TL-DNA, the T-DNA of type II and type III pRi, and the 15th ORF of type I pRi, according to Hooykaas and Hooykaas (2021). The *rolA* gene has cis-regulatory elements, including the promoter, 5′- and 3′-UTRs, and polyadenylation sites, in addition to the coding region (CDS) (Sinkar et al. 1988). The length of ORF10 in various *R. rhizogenes* strains ranges from 279–423 bp, according to recent and past studies of *rolA* gene structure. The *rolA* promoter is thought to be phloem specific (Schmülling et al. 1989). Subsequent investigations have shown that the *rolA* transcripts of *Arabidopsis* plants contain both 5′- and 3′-UTRs, with the 5′-UTR displaying traits typical of plant precursor RNA introns that differ between mannopine and agropine pRi (Magrelli et al. 1994). Moreover, the splicing of *rolA* mRNA is necessary for efficient in vivo expression of the *rolA* phenotype (Spena and Langenkemper 1997). Xue et al. (2008) conducted a comparative analysis of *rolA* splicing in transgenic tobacco, apple, and *Arabidopsis*. The introns ranged in length from 84 to 75 bp, whereas the 3′-UTR was 549 bp long. The RolA proteins from all three types of Ri plasmids are small (approximately 100 amino acid residues) and have a high pI (more than 11). Investigations of the N-terminus of A4-RolA have shown its essential role in its biological function. Additionally, a highly hydrophobic region was found (Barros et al. 2003). Bioinformatics analysis of the RolA protein structure was performed by Rigden and Carneiro (1999). They considered it the most appropriate comparative model of RolA on the basis of the papillomavirus E2 (2bopA) domain structure. This model suggests that RolA is a DNA-binding protein or a transcription factor.

RolA may be essential for the biochemical pathways involved in the development of hairy root symptoms. Plants with pRi morphology can be classified into two categories: those with transformed phenotypes (T) and those with super-transformed phenotypes (T′). T-phenotype plants present fewer pRi-induced symptoms (Tepfer 1984). The antagonism between *rolA* and *rolB* is typically the reason for the smoothing of the traits of pRi-phenotype T. Moreover, one of the main functions of *rolA* is to regulate the expression of *rolB*. One such instance that produces an antisense message is the finding of additional *rolA* transcripts, which span the whole *rolB* sequence and have a size range of 2.1–2.8 kb (Durand-Tardif et al. 1985). The expression of the *rolB* gene has been shown to be strongly controlled by the ACTTTA motif, which binds to transcription factors such as NtBBF1 with Dof domains (Baumann et al. 1999). The expression of the *rolB* gene is dose-independently correlated with the presence of auxin throughout a 48 h period; however, the expression of this transcription factor is not auxin dependent (Baumann et al. 1999). A possible explanation for the combined effect on the ROS signalling system has been presented recently. It was shown that *rolB* (Veremeichik et al. 2016) and *rolC* (Shkryl et al. 2022) are responsible for the upregulation and downregulation of *Rboh* gene expression, respectively. Individual expression of the *rolB* and *rolC* genes also differentially affects the expression of the ROS scavengers (Bulgakov et al. 2012; Shkryl et al. 2022). According to Maurel et al. (1991), RolB is known to induce sensitivity to exogenous auxin, which is followed by necrosis and growth inhibition (White et al. 1982; Schmülling et al. 1988). Conversely, *rolA* gene expression leads to a decrease in endogenous IAA (Dehio et al. 1993; Bettini et al. 2016). Knowledge of the ROS steady state is lacking, which makes it difficult to comprehend how RolA regulates physiological

activities. Furthermore, it is still unclear how exogenous auxins control the individual expression of the *rolA* gene.

In 2000, *R. cordifolia rolA*-transformed callus cultures (RA cultures) were obtained (Shkryl et al. 2008). Over the first 14 years, the expression of the *rolA* gene showed only a slight effect on secondary metabolism. Anthraquinone (AQ) production was three times greater than that in untransformed callus cultures. Nonetheless, a sudden increase in the AQ content in the RA calli line was observed in 2014 (Veremeichik et al. 2019). The production of AQs increased to 874 mg/L, which was ten times greater than the AQ content in the control culture (Veremeichik et al. 2019). Numerous hypotheses have been proposed for the possible causes of the sudden AQ biosynthesis activation. Among them is the possibility that changes in the nucleotide sequence of the *rolA* oncogene could have occurred during a period of long-term cultivation. An in-depth analysis of the coding and cis-regulatory elements of the *rolA* gene has revealed a new direction for research. In the present study, we investigated the effects of IAA on *rolA* gene expression and ROS homeostasis in *rolA*-transformed cells.

Materials and methods

Callus cultivation and auxin treatments

A nontransgenic cell culture of *R. cordifolia* was previously obtained from a plant collected in the southern area of Primorsky Krai, Russia. In this study, the nontransgenic control culture was denoted by R (Mischenko et al. 1999). This culture was subsequently transformed via the *rolA* gene (GenBank: K03313.1), as previously reported by Bulgakov et al. (2002), under the control of its own native promoter (Shkryl et al. 2008). The calli line was identified as RA in this investigation. For over two decades, *R. cordifolia* cultures transformed with the *rolA* gene and the control culture R have been cultivated under the following conditions: calli are subcultured every 30 days in the dark on agarized media. For R calli, 0.5 mg/l 6-benzylaminopurine and 2.0 mg/l α-naphthaleneacetic acid were added to the media. The plant growth regulators (PGR)-containing medium used in this study was called W/BA. Hormone-free media (W0) was used for cultivating the *R. cordifolia rolA*-transgenic callus lines.

Obtaining a genetic construct and transformation of a cell culture

To obtain the new *rolA*-harvesting genetic construct, the *rolA* gene (GenBank: K03313.1) under the control of its own native promoter was amplified using primer pairs listed in Suppl. Table S1. The PCR product and the pSAT6 cassette vector were digested with *Age*I and *Apa*I enzymes (NEB, Ipswich, MA, USA) at 5′-ACCGGT-3′ and 5′-GGGCCC-3′, respectively, and ligated according to the manufacturer's protocol (NEB). The resulting construct, pSAT6-*rolA*Prom-*rolA*, was sequenced to check its integrity. Next, the *rolA*Prom-*rolA*-terminator was transferred from the pSAT6 vector via the PI-*Psp*I (NEB) enzyme into the pPZP-RCS2 expression binary vector containing the kanamycin resistance gene (*nptII*) (Tzfira et al. 2005). The resulting binary vector was subsequently transformed into *Agrobacterium tumefaciens* strain EHA105 cells (Hood et al. 1993) via electroporation (GenePulser, Bio-Rad, Hercules, CA, USA). The obtained recombinant strain of *Agrobacterium* was used for the genetic transformation of *R. cordifolia* control cell cultures, as described previously (Shkryl et al. 2011). A transgenic culture, designated RAN (Rubia rolA New), was obtained after six months of selection on kanamycin. The callus cultures were successfully cultivated on both W/BA and W0 media in the dark at 24 °C with 28-day subculture intervals.

HPLC–PDA-MS determination of anthraquinones (AQs)

The callus extracts for the HPLC assay were prepared by ultrasonic treatment of dried and ground tissue in 80% methanol and cleared with a 0.45-µm membrane (Millipore, Bedford, MA, USA).

Both HPLC–PDA and HRMS studies were performed for AQ determination. An Agilent 1260 Infinity instrument (Agilent Technologies, Santa Clara, CA, USA) fitted with a PDA detector was used for analytical HPLC metabolite profiling. An analytical Zorbax C18 column (150 mm, 2.1 mm i.d., 3.5 µm part size; Agilent Technologies) heated at 40 °C was used as the stationary phase. A binary gradient with A (0.1% aqueous formic acid) and B (acetonitrile with 0.1% formic acid addition) was installed with a flow rate of 0.2 ml/min, starting at 0% B. The following linear gradient profile was used: 0–35 min – 0–40% B; 40 min – 50% B; 50 min – 100% B. UV/Vis spectra for each individual peak were captured between 200 and 800 nm using a PDA detector. The wavelength of 430 nm was chosen for recording the chromatograms for AQ determination. A Shimadzu LCMS-IT-TOF instrument (Shimadzu, Kyoto, Japan) including a tandem ion trap/time-of-flight mass spectrometer was used for the high-resolution MS studies. Electrospray ionisation (ESI) was used in both positive and negative ion modes. The MS conditions were as follows: the range of *m/z* detection was 100–1200, the drying gas (N_2) pressure was 150 kPa, the nebuliser gas (N_2) flow rate was 1.5 l/min, the ion source potential changed from − 3.8 to 4.5 kV, and the interface

temperature was 200 °C. Additionally, MS^2 data were collected in automatic mode.

RNA isolation, cDNA synthesis and real-time PCR

DNA and RNA extraction

DNA from fresh and dried tissue of cell cultures was isolated using the SDS buffer method (Chabi Sika et al. 2015). DNA quality was assessed by gel electrophoresis on a 0.8% agarose gel in the presence of ethidium bromide. The isolated DNA was diluted 50 times or more. To analyse *rol*A and ROS-generated/scavenging gene expression, samples of R, RA, and RAN cultures were harvested from 30-day-old cell cultures. For all RT analyses, we used three independent RNA extractions. Isolation of total RNA and first-strand cDNA synthesis were carried out as described previously (Shkryl et al. 2008). All RNA samples were treated with DNAse (Biolabmix, Novosibirsk, Russia) according to the manufacturer's protocol.

Cloning of rolA mutants

The PCR products were obtained from the DNA of the *rolA*-transformed cultures with specific primers targeting the promoter and 3′-untranslated regions of the *rolA* gene (Suppl. Table S1). PCR was performed using a kit for the amplification of complex plant DNA regions using high-precision and high-throughput Phire polymerase, which also detects potential mutations and removes PCR errors, and 2X PCR buffer according to the manufacturer's protocol (Thermo Fisher Scientific, Waltham, MA, USA). The reaction was carried out in an iCycler amplifier (Bio-Rad Laboratories) programmed for the following reaction conditions: preliminary denaturation at 95 °C for 3 min; 35 cycles of 95 °C for 30 s, 55 °C for 20 s, and 72 °C for 60 s; and final elongation at 72 °C for 3 min. For cloning, the PCR products were purified by isolation with a low-melting agarose gel (Sigma-Aldrich, Burlington, MA, USA) using phenol extraction (Sambrook et al. 1989). The purified PCR products were cloned and inserted into the pJET vector using the CloneJET PCR Cloning Kit (Thermo Fisher Scientific), and the resulting ligation mixture was used to transform the *E. coli* Turbo strain (NEB). The sequencing reaction was performed using the BigDye Terminator Cycle Sequencing Kit (Applied Biosystems, Woburn, MA, USA) in an iCycler cycler programmed for the following reaction conditions: predenaturation at 96 °C for 1 min; 30 cycles of 96 °C for 20 s, 55 °C for 20 s, and 60 °C for 3 min. The sequence was determined using the ABI 3500 Genetic Analyser (Applied Biosystems) at the Instrumental Centre of Biotechnology and Gene Engineering of FSCEATB FEB RAS. At least 150 individual clones of DNA obtained from RA cultures in 2008 and 2024 were analysed. The search for homologues of sequenced DNA fragments was carried out in the GenBank sequence database using the BLAST program (Altschul et al. 1990). Amino acid sequences corresponding to the sequenced cDNA fragments were determined using the GeneRunner v3.0 program.

Design of primers for real-time PCR

Primers for the evaluation of *rolA* expression with point mutations were developed using the technique described by Hayashi et al. (2004). The direct primer, in addition to the substitution at the last 3′ position, also had an artifact substitution at the 3rd position from the 3′ end. In this case, artefact replacement was performed according to the principle of A/T → G or G/C → A nucleotides (Suppl. Fig. S1a). All primers used are listed in Suppl. Table S1.

Real-time PCR

The expression of the genes encoding the ROS-generating enzymes (NADPH-oxidase, RcRboh3), the enzymes responsible for ROS detoxification (catalase, RcCat; superoxide dismutases, RcCSD1-3; ascorbate peroxidases, RcApx1-3, Shkryl et al. 2010), and housekeeping reference genes such as actin and 18 s (Shkryl et al. 2011) were examined using the previously described gene-specific primer pairs. A CFX96 instrument (Bio-Rad Laboratories) was used with 2.5 × SYBR Green PCR Master Mix (Biolabmix) for quantitative real-time PCR (qPCR) examination. Three biological and three technical replicates from three distinct RNA extractions were used for analysis. A 10 µl volume containing 250 nM of each primer, 1 µl of the diluted cDNA sample, and 2 mM $MgCl_2$ was used for the reactions. To confirm that there was no contamination, qPCR analysis was performed with both the RNA-RT and no-template controls. CFX Manager Software (Version 1.5; Bio-Rad Laboratories) was used to analyse the data. Using the formula $2^{-\Delta\Delta Ct}$, the lower-expressing sample was given a value of 1 in the relative mRNA calculation. CFX Manager software (version 1.5; Bio-Rad Laboratories, Inc.) was used to analyse the data. qPCR analysis for the detection of mutant genes on the basis of melting curves was performed on a CFX96 instrument (Bio-Rad) with 2.5 × SYBR Green PCR Master Mix (Biolabmix) in accordance with the manufacturer's protocol. The reaction conditions were as follows: preliminary denaturation at 95 °C for 3 min; 35 cycles at 95 °C for 20 s, 60 °C for 20 s, and 72 °C for 30 s; final elongation at 72 °C for 3 min; denaturation at 95 °C for 10 min; and melting curves in the range of 75–90 °C with a temperature increase of 0.2 °C, with 100 repetitions. To verify that there were no nonspecific products or primer−dimer artefacts in the samples, melting curve analysis and product visualisation via electrophoresis

on a 1% agarose gel stained with ethidium bromide were employed. The results were analysed by using Bio-Rad CFX Manager software (Version 3.1; Bio-Rad Laboratories).

Laser confocal imaging of intracellular ROS in living cells

The intracellular ROS abundance was measured using a previously described methodology (Veremeichik et al. 2021). The foundation of these investigations is the capacity of plant cells to oxidise fluorogenic dyes to their corresponding fluorescent equivalents. Callus cultures (R, RA, and RAN) that were 30-day-old, stable, or had grown on acidified W/BA or W0 for one passage were stained for 10 min at 25 °C in the dark with 2,7-dichlorodihydrofluorescein diacetate (H2DCF-DA, Molecular Probes, Eugene, OR, USA) at a final concentration of 50 µg/ml. After two rounds of washing, the DCF fluorescence levels within the cells were promptly assessed using an argon laser (λex = 488 nm; emission Ch3-LP filter, 505 nm) and an Axiovert 200 M LSM510 META confocal microscope (Zeiss, Oberkochen, Germany). Using LSM 510 software release 4.2 (Zeiss), time series files were obtained and stored on a computer hard disc. The data are presented as the average of six different tests, each of which involved the analysis of at least thirty to forty cells.

Statistical analysis

All values are presented using Statistica 10.0 (StatSoft Inc., USA) as the mean ± SE. A significant difference was defined as $P < 0.05$. Student's t test was used to compare two independent categories, and ANOVA and multiple comparisons were used to evaluate data across multiple groups. For the intergroup comparisons, Fisher's protected least significant difference (PLSD) post hoc test was used.

Results

Identification of SNPs in the rolA gene of long-term cultivated rolA-transgenic calli of R. cordifolia

Numerous hypotheses have been proposed for the potential causes of sudden AQ biosynthesis activation. Among them is the possibility that changes in the nucleotide sequence of the *rolA* oncogene could have occurred during a period of long-term cultivation. To investigate this theory, DNA was extracted from dried RA culture tissue that was obtained in 2008, prior to modifications in the biosynthetic status, and from fresh tissue. For the DNA template, the whole *rolA* gene, including its promoter and 5′ and 3′ untranslated regions, was amplified using the highly precise and effective polymerase. The PCR products were subsequently cloned and inserted into pJET vectors. For each of the variants (DNA 2008 and DNA 2024), at least 150 clones were sequenced. Sequencing the PCR products yielded the following results. The promoter region sequence was unchanged for both 2008 and 2024 DNA. Moreover, we detected and recognised the native motif (Fig. 1a, designated a black triangle) of the auxin-dependent Dof protein (Baumann et al. 1999).

In the 2008 DNA template, no changes were detected in the nucleotide sequence of the *rolA* gene. In the 2024 DNA matrix, 8 clones were found to contain various mutations. By analysing the obtained clones, we identified two groups of mutations (Fig. 1, Suppl. Fig. S2): mutations in the

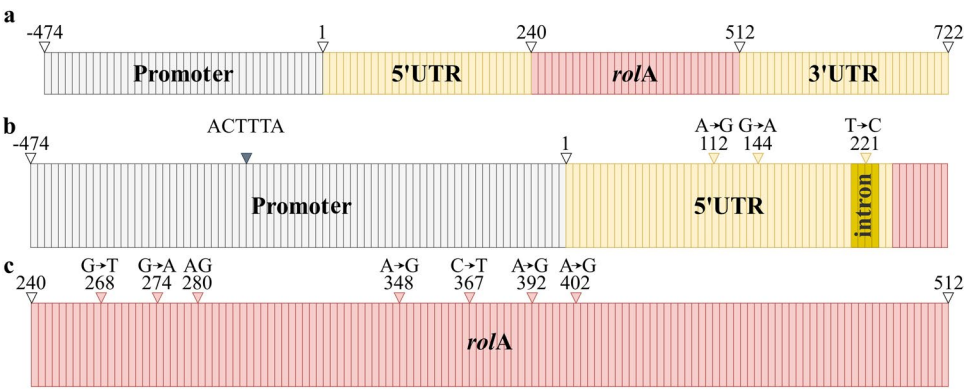

Fig. 1 Simplified diagrams of the structure of the *rolA* gene based on pRiA4 plasmids and the detected substitutions. The simplified scheme (**a**) of the main parts of the *rol*A gene is represented: promoter (−474–1 bp), grey block; 5′- and 3′-UTRs (1–240 and 512–722 bp, respectively), yellow blocks; *rol*A coding region (240–512 bp), pink block (accordingly to Spena and Langenkemper 1997; Pandolfini et al. 2000; Xue et al. 2008). The detected substitutions in 5′-UTR (**b**) are designated yellow triangles; the motif (ACTTTA) for the auxin-dependent Dof protein is designated a grey triangle (Baumann et al. 1999); the intron is designated deep yellow blocks. The detected substitutions in the the *rol*A coding region (**c**) are designated pink triangles, respectively

5′-untranslated region (AMU) and mutations in the coding region of the gene (AMC). As shown in Fig. 1b, the detected substitutions in the 5'-UTR and in the *rol*A coding region are designated yellow and pink triangles, respectively. Three variants of AMU-type mutations were found: AMU1 (substitution of A to G at position 112), AMU2 (substitution of G to A at position 144), and AMU3 (substitution of T to C at position 221). Five variants of AMC-type mutations were identified: AMC123 (3 consecutive nucleotide substitutions A to G at positions 280, 348, and 403), AMC4 (substitution A to G at position 392), AMC5 (substitution G to T at position 268), AMC6 (substitution G to A at position 274), and AMC7 (substitution C with T at position 367). Nucleotide substitutions in AMC lead to changes in the amino acid sequence of the RolA protein.

The next step in our work was to confirm the presence of mutations detected during sequencing via PCR with specific primers. For this purpose, artificial forward primers were developed for each mutation variant. The mechanism of operation of artificial primers is as follows (Hayashi et al. 2004): a primer containing a substitution corresponding to the mutation as the last nucleotide and an artifact substitution nucleotide (i.e., substitution of A/T for G/C and vice versa) acquires increased specificity for the mutant sequence and loses the ability to anneal to the native gene. PCR with such a primer paired with a specific reverse primer will yield a product only on the SNP-containing template. For each mutant sequence, we developed a forward primer with two described substitutions; a common primer was used as a reverse primer. Analysis of the selective efficiency of primers by PCR with visualisation of reaction products in agarose gel (Suppl. Fig. S1b) revealed that the combination of primers, in which a specific artificial forward primer is used for each specific mutation, resulted in an equivalent concentration of a plasmid containing the native form of the *rolA* gene (AWT) and plasmids containing the corresponding mutation, and the PCR product was visible only on the mutated plasmid (Suppl. Fig. S1).

There are incredibly few copies of the transgene in the genomes of plant cells. We employed real-time PCR with melting curve product detection to identify transgene mutants. Suppl. Fig. S3 shows that none of the mutations were found on the 2008 RA DNA template. Additionally, the RA 2024 DNA matrix showed evidence of all 8 mutations (Suppl. Fig. S3, red asterisks). Two mutations, AMU1 and AMC6, were weakly detected on the cDNA template (Suppl. Fig. S3, green asterisks). Despite the reliability of the results obtained, owing to the extremely weak level of expression, it is difficult to assume that the detected mutations could be the cause of the biochemical changes in long-cultivated *rolA*-transformed cultures.

Auxin-mediated expression of the rolA gene in transformed R. cordifolia callus cultures

In the promoter region of the *rolA* gene, we detected and recognised a native motif (Fig. 1a, designated a black triangle) for the auxin-dependent Dof protein, which was previously described for the *rolB* gene (Baumann et al. 1999). We hypothesised that *rolA* gene expression may be regulated by auxins. To determine how auxin affects *rolA* gene expression and related processes, we obtained a new *rolA*-transformed *R. cordifolia* cell culture. We compared the effects of exogenous auxins on growth and transgene expression in both callus cultures. We obtained a new genetic construct based on the pSAT16 vector, which carries the *rolA* gene under the control of its own promoter (Fig. 2a). The cassette vector pSAT16 containing *rolA* was obtained according to the description in Materials and methods. The genetic construct *rolA*-Promoter-*rolA*−35S terminator was transferred into the binary vector pPZP (Suppl. Fig. S4). The binary vector was then transferred into the *A. tumefaciens* strain EHA105 by electroporation. The control *R. cordifolia* cell line, designated R, was transformed via *Agrobacterium*-mediated transformation. After selection on kanamycin-supplemented media (50 mg/l) for six months, kanamycin-resistant callus lines were obtained and designated RAN (Rubia-*rolA*-New). While the control cell culture had a yellow color, the new *rolA*-transformed cell cultures had a similar morphology, with a deep yellow tint and a friable consistency (Fig. 2b).

The long-term cultivated RA cell line was subsequently grown on PGR-free media. In the presence of hormones, the growth of the culture decreased after several passages; however, the growth was stable. In the absence of hormones, the control culture R completely died after the second passage. The new *rolA*-transformed callus culture RAN was grown with (W/BA media) and without PGR (W/0 media). The growth of cell culture RAN was similar to that of RA; PGR led to slight decreases in growth (Fig. 2c). To confirm successful *rolA* gene expression and the effect of exogenous auxins, new RAN and long-term cultivated callus culture RA were grown in the presence of IAA (2 mg/l). Analyses of the *rolA* gene expression were performed on the 1st, 15th, and 30th days of growth, and the results were compared with those of PGR-free growing cells using qPCR with a melting curve. The *rolA* gene expression was significantly greater in the RAN cell line than in the RA line when the cultures were grown on PGR-free media. When IAA was added, *rolA* gene expression increased in both cell lines after 30 days of treatment (Fig. 2d). Thus, in long-term cultivated cell lines, the abundance of the transgene may have decreased. However, the ability of the RA cell culture to grow in a PGR-free medium ensures the safety of the transgene as a selective marker.

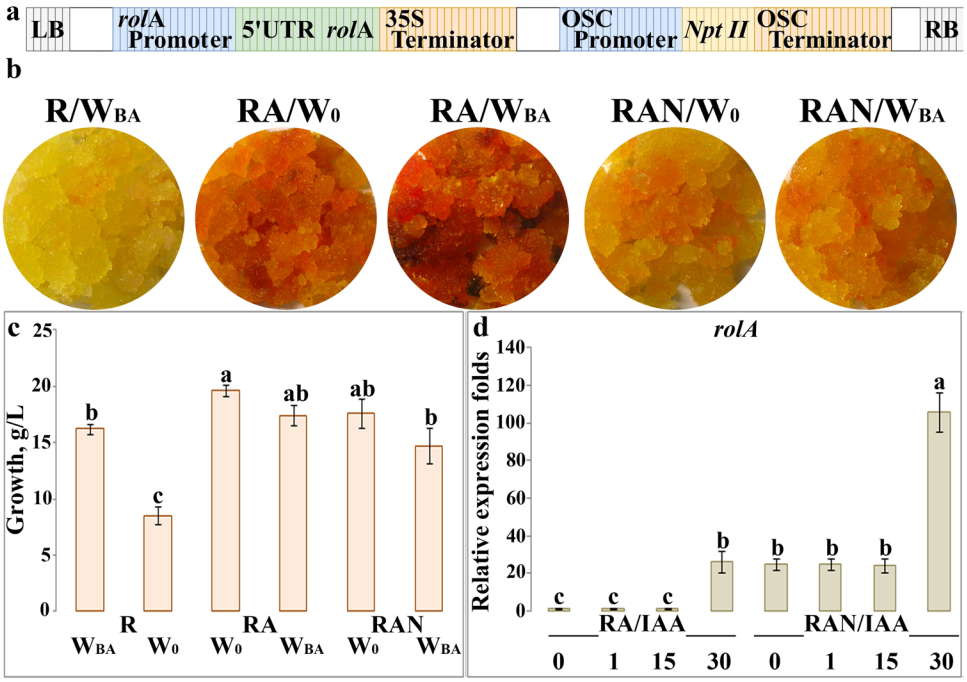

Fig. 2 Generation and comparative analysis of a new *rolA*-transformed callus culture of *R. cordifolia*. **a** Description of the genetic construct. Right border: T-DNA part of the pPZP vector, RB, LB. Left border: *rolA*'s promoter and 35S term, 35S cauliflower mosaic virus terminator; 5'UTR *rolA*, part of the *rolA* gene including coding region and 5' untranslated regions; Ocs Prom/Term, the octopine synthase promoter/terminator; *nptII*, neomycin phosphotransferase II. **b-d** Phenotypes (**b**), growth (**c**), and *rolA* gene expression (**d**) of the control (R), long-term cultured (RA) and newly obtained (RAN) *rolA*-transformed callus cultures of *R. cordifolia*. R, control cell culture stable growing on W/BA media; RA and RAN, *rolA*-transformed cell cultures stable growing on W0 and W/BA media, respectively. The data are presented as the mean ± SE from four subcultures (biological replicates) with two technical replicates for each experiment. Different letters above the bars indicate statistically significant differences ($P < 0.05$, Fisher's LSD)

Analysis of the AQ content

First, the callus lines of *R. cordifolia* were analysed using HPLC–PDA-MS. The chromatographic separation of the AQs is shown in Fig. 3a, b. A total of 12 major peaks of AQs were detected and tentatively identified. UV−Vis and mass−spectral data were collected and examined. We obtained high-resolution mass measurements and developed molecular formulas for the detected compounds with mass measurement uncertainties of less than 4.5 mDa. All the data required for identification are listed in Suppl. Table S2. Thus, peaks 1–5 were identified as follows: pseudopurpurin primveroside (1), pseudopurpurin glucoside (2), munjistin glucoside (3), lucidin primveroside (4) and ruberitrinic acid (5), as we reported previously (Shkryl et al. 2016). Additionally, two peaks (11 and 12) corresponded to AQ aglycones (Shkryl et al. 2016). Therefore, peak 11, with a retention time of 37.5 min, was defined as the sum of three undivided components: alizarin ($[M\text{-}H]^-$ at *m/z* 239), munjistin ($[M\text{-}H]^-$ at *m/z* 283) and pseudopurpurin ($[M\text{-}H]^-$ at *m/z* 299) (Suppl. Table S2, and Suppl. Fig. S5). Peak 12, with a retention time of 40.8 min, was identified as purpurin ($[M\text{-}H]^-$ at *m/z* 255) (Shkryl et al. 2016). In addition, at least five new components were recognised as AQ derivatives to coincide with previously published data for Rubiaceae (Tripathi et al. 1997; Derksen et al. 2002; Boldizsar et al. 2006). Thus, the following AQ derivatives were tentatively determined: alizarin-methyl ether gentiobioside (peak **6**, $[M\text{-}H]^-$ at *m/z* 577), lucidin glucoside (peak **7**, $[M\text{-}H]^-$ at *m/z* 431), alizarin-methyl ether primveroside (peak **8**, $[M\text{-}H]^-$ at *m/z* 547), purpurin-methyl ether primveroside (peak 9, $[M\text{-}H]^-$ at *m/z* 563) and rubiadin primeveroside (peak 10, $[M\text{-}H]^-$ at *m/z* 547) (Suppl. Table S2).

As shown in Fig. 3a, b, and Suppl. Table S3, the extract of R calli contained only compounds 1–3 and 11, whereas all 12 compounds were detected in the long-term-cultivated *rolA*-transformed calli of RA. In addition to the four minor compounds 7–10, eight other major AQ derivatives were found in the extract of the newly obtained *rolA*-transformed calli RAN (Fig. 3a, Suppl. Table S3). A semi-quantitative evaluation of the AQ content was carried out to compare the samples with each other in terms of peak areas (recorded at a wavelength of 430 nm). An analysis of the AQ content revealed that the relative AQ content was 2.4- and 35-fold greater in the *rolA*-transformed calli (for the RAN and RA callus lines, respectively) than in the control R calli (Fig. 3c).

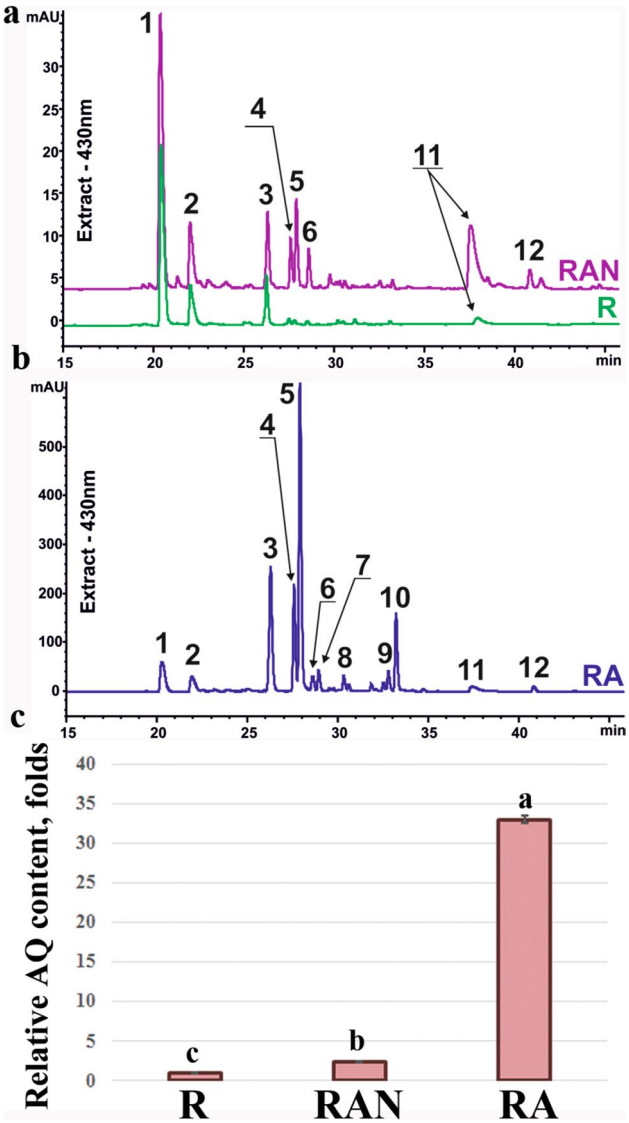

Fig. 3 **a** HPLC (430 nm) anthraquinone (AQ) profiling comparison of the crude extracts obtained from R (control cell culture) and *rolA*-transformed newly obtained (RAN) culture. **b** Long-term cultured (RA) callus cultures of *R. cordifolia*. The peak numbers correspond to those listed in Suppl. Table S1. **c** Relative AQ content in R (control cell culture), *rolA*-transformed newly obtained (RAN) culture, and long-term cultured (RA) callus cultures of *R. cordifolia* was calculated as a semi-quantitative evaluation of peak areas obtained from each chromatogram (recorded at a wavelength of 430 nm). The control calli R were stably grown on W/BA media, and *rolA*-transformed calli were stably grown on W0 media for 30 days. The data are presented as the mean ± SE from four subcultures (biological replicates) with two technical replicates for each experiment. Different letters above the bars indicate statistically significant differences ($P < 0.05$, Fisher's LSD)

ROS accumulation in the control and rolA-transformed R. cordifolia callus cultures

The reactive oxygen species are important mediators of numerous plant cell processes, including development, growth, and stress responses. These cellular processes require a basal ROS level. An increase in ROS triggers stress responses, such as the production of specialised metabolites, and an excess of ROS causes oxidative stress, which is lethal (Mittler 2017). Individual expression of *rolB* and *rolC* has been demonstrated to be able to regulate ROS generation, accumulation, and scavenger expression (Bulgakov et al. 2008, 2012, 2013; Veremeichik et al. 2016; Shkryl et al. 2022). In a previous study, we reported PGR-dependent modulation of *rolA* and *rolB* gene expression, intracellular ROS levels and the expression of genes involved in ROS metabolism in pRiA4-transformed calli (Veremeichik et al. 2023b).

We compared *R. cordifolia* control untransformed cell cultures and both recently obtained (RAN) and long-term cultured (RA) *rolA*-expressing cell cultures. We analysed the following variants: *rolA*-transformed callus cultures were grown on the comfortable PGR-free W0 for 30 days, and R was stably grown on W/BA and W0 for 30 days. Using confocal microscopy, the fluorescence of individual live cells loaded with H2DCF-DA was quantified. The accumulation of intracellular ROS in the R cells was monitored, and the results revealed that the ROS levels in the developing R cells were equal to those in the W/BA and W0 cultures (Fig. 4). Compared with those in control R calli, a significant decrease of 20% in the level of intracellular ROS was detected in both long-term cultured RA and newly obtained RAN calli. In general, ROS accumulation was equal in both RA and RAN calli (Fig. 4).

Expression of ROS metabolism enzymes in the control and rolA-transformed callus cultures of R. cordifolia

Singlet oxygen radicals (SORs) are produced by the Rhoh protein (Fig. 5, left panel; Mittler 2017). We previously demonstrated that stress induces *RcRboh1* expression (Veremeichik et al. 2016). Furthermore, overexpression of the *rolB* gene increased the expression of the *RcRboh1* gene, but overexpression of the *rolC* gene had the opposite effect (Veremeichik et al. 2016; Shkryl et al. 2022). In the present study, we analysed the expression of the *RcRboh1* gene in

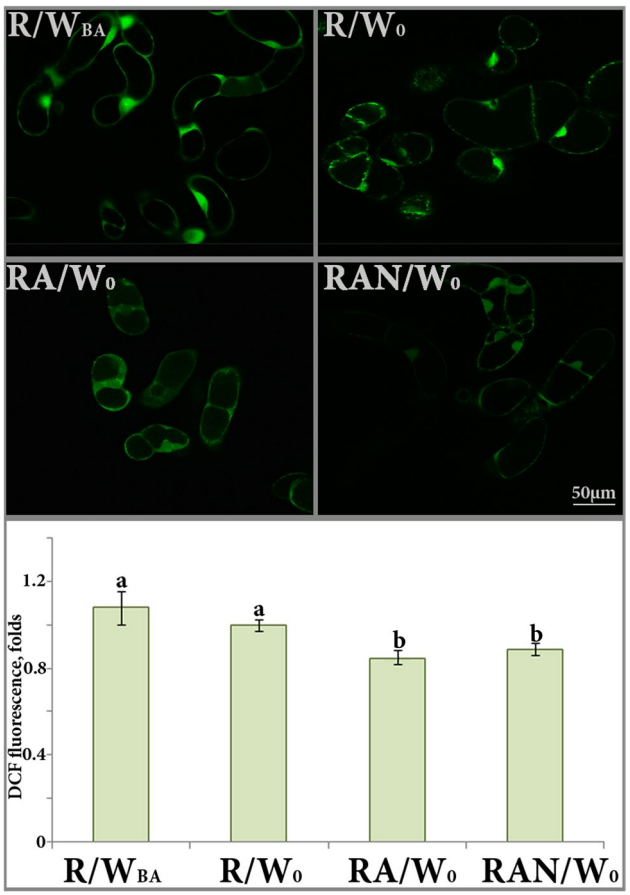

Fig. 4 **a, b** ROS accumulation in *R. cordifolia* cells was measured via confocal microscopy (**a**) and DCF fluorescence (**b**). Abundance of intracellular reactive oxygen species (ROS) in R, control cell culture stable growing on W/BA media and growing on W0 media for one passage; long-term cultured (RA) and newly obtained (RAN) *rolA*-transformed callus cultures of *R. cordifolia*, stable growing on W0 media. The ROS levels are presented as the mean ± standard error from six independent experiments at the end phase of growth (30 days). Different letters above the bars indicate statistically significant differences ($P < 0.05$, Fisher's LSD)

long-term cultivated *R. cordifolia* and newly obtained *rolA*-transformed *R. cordifolia* cell cultures in comparison with the control untransformed cell cultures.

We compared the 30-day-old callus lines: R stable growing on W/BA and *rolA*-transformed callus cultures stable growing on the comfortable PGR-free W0 for 30 days and growing on media supplemented with IAA for 30 days. The expression of the stress-induced *RcRboh1* gene was strongly lower in *rolA*-expressing calli than in control R calli. IAA treatment enhanced this effect (Fig. 5**,** right panel, top). In addition, at the end of growth, the expression patterns of the ROS-scavenging enzymes (*RcCSDs*, *RcApxs*, and *RcCat*, Fig. 5, left panel; Mittler 2017) were measured. The expression of all three *RcCSD* genes was reduced in *rolA*-expressing calli. The level of expression of *the RcApx1* gene was equal in the control and *rolA*-expressing calli, whereas the expression of the stress-induced *RcApx2* and *RcCat1* genes was lower in the *rolA*-expressing calli than in the control calli. IAA treatment enhanced this effect (Fig. 5, right panel, bottom).

Discussion

The wild-type pRi-expressing plants presented a variety of characteristics, including decreased apical dominance, shorter internodes in roots, taller nodes, shoots, and root branching, wrinkled, dark-green leaves, enhanced secondary metabolites, and a changed essential oil composition. A comprehensive investigation of the biological function of *rol* genes in natural transformants, as well as their presence in the genomes of certain plant species (Matveeva and Otten 2019, 2021; Stavnstrup et al. 2020; Chen et al. 2022), has revealed significant advantages of *rol* gene expression on a number of physiological processes, such as metabolism, the induction of aberrant growth, and the rerouting of growth of roots and other plant organs (Desmet et al. 2021). Several of these characteristics may be helpful in crop breeding and selection (Desmet et al. 2020b). A common application of wild *R. rhizogenes*-mediated transformation is the production of phytochemical compounds for pharmaceuticals. Understanding the biological function of each *rol* gene in this complex process is essential. However, as previously indicated, most studies on the biological roles of *rol* genes have been carried out in agropine strains, most notably the A4 strain. Therefore, we may discuss the role and potential biological relevance of the agropine *rolA* gene, which has a frameshift that could make it different from *rolA* in other pRi types (Veremeichik et al. 2023a). The overexpression of the A4-*rolA* gene results in a number of traits, including reduced size (Holefors et al. 1998; Zhu et al. 2001; Zia et al. 2010), resistance to *Fusarium oxysporum* and a reduction in ABA and IAA (Bettini et al. 2016), and wrinkled leaves (Sinkar in 1988). Another important effect of A4-*rolA* gene expression is the induction of specialised metabolism in tobacco root cultures (Palazon et al. 1997), *R. cordifolia* cell cultures (Shkryl et al. 2008), and *Artemisia dubia* plants (Amanullah et al. 2016). A study by Serino et al. (1994) examined a *rolA* homologue that was isolated from cucumopine pRi (*rolα*). The similarity between *rolα* and *rolA* is lower than that of other *rolA* genes. The hairy root syndrome is caused by more effective stimulation of root growth caused by *rolα* (Serino et al. 1994). However, despite the effects shown, the function of the *rolA* gene remains unknown. This is why the *plast* gene group does not contain *rolA*. There is a fourth category of "orphan genes", which includes T-DNA genes with unclear functions, such as *rolA* (Otten 2018a). In the present work, we tried to clarify two phenomena shown in

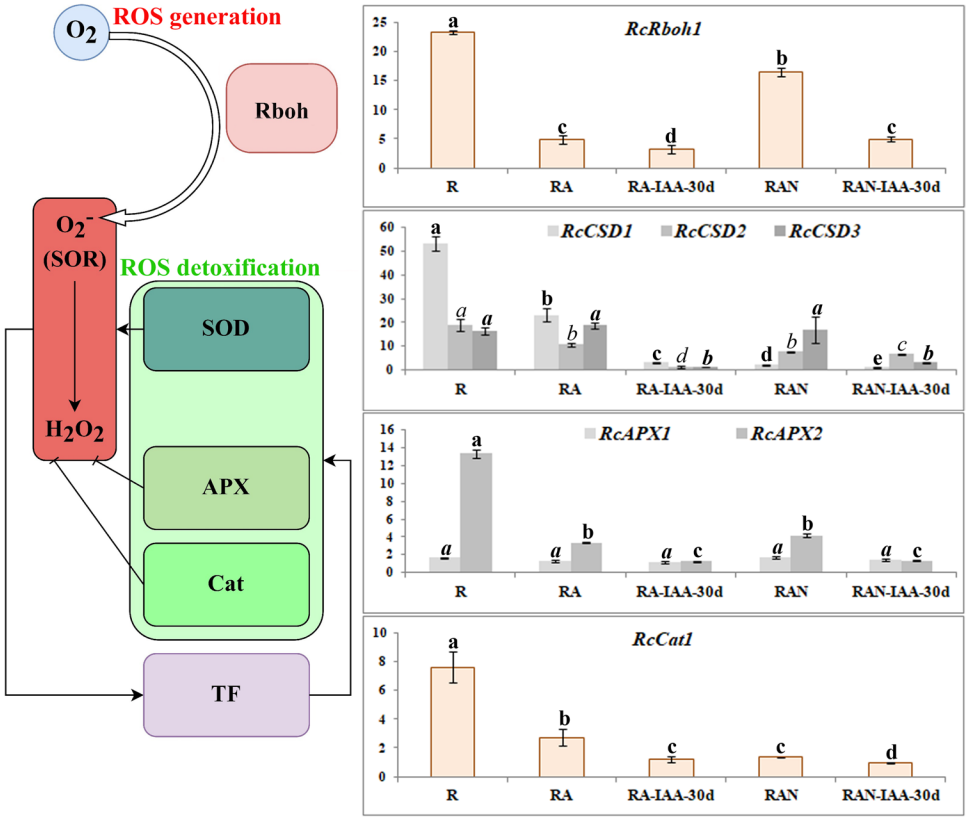

Fig. 5 Expression of ROS metabolism enzymes in the control and *rolA*-transformed callus cultures of *R. cordifolia*. R, control cell culture stable growing on W/BA media and growing on W0 media for one passage, long-term cultured (RA) and newly obtained (RAN) *rolA*-transformed callus cultures of *R. cordifolia*, stable growing on W0 media and growing on W/BA media for one passage. The left block of the figure is a scheme (Mittler 2017) of the generation of singlet oxygen radicals (SORs) by Rboh enzymes and, below, the ROS detoxification system, including ROS-scavenging enzymes (SOD, superoxide dismutase; APX, ascorbate peroxidase; Cat, catalases) and their ROS-activated transcription factors (TFs). The right block presents the mRNA levels measured by real-time PCR and is reported as the relative expression of the *Rboh* gene and genes encoding antioxidant enzymes. The analysis was repeated three times; 30-day-old cell cultures were used. The data are presented as the mean ± standard error. Different letters above the bars indicate significantly different means ($P < 0.05$; Fisher's LSD)

previous studies. (1) What led to the activation of secondary metabolism in long-term cultivated *rolA*-transformed *R. cordifolia* cell cultures? (2) What effect does *rolA* gene expression have on ROS metabolism?

Calli of *R. cordifolia* transformed with the *rolA* gene have been cultivated for more than 14 years. Since 2014, *rolA*-transgenic culture has altered the biosynthesis of the secondary metabolite AQs. Moreover, the control culture did not undergo any changes (Veremeichik et al. 2019). The expression of the *rolA* gene in the transformed culture was stable during cultivation. However, a change was found not only in metabolism but also in the expression of key genes encoding enzymes involved in AQ biosynthesis. The reason for this shift may be the appearance of a SNP in the *rolA* gene as a result of long-term cultivation. In the present work, an in-depth analysis revealed the appearance of SNPs both in the coding region and in the 5' UTR. However, analysis of the SNP expression data revealed that the expression of these forms was negligible compared with that of the native *rolA* gene. In addition, the detected mutations do not affect known essential amino acids of the RolA protein, such as D0, D7, B12, B17, S23, K24, R27, R28, K32, R33, R43, N51, and S80 (Rigden and Carneiro 1999). Thus, it can be assumed that the accumulation of mutations is not associated with the biosynthetic shift, and it is necessary to look for another reason.

An important result of this research is the discovery of the sequence of the ACTTTA motif in the promoter region of the *rolA* gene. This motif binds IAA-mediated transcription factors such as NtBBF1, which contains Dof domains, as described for the *rolB* gene (Baumann et al. 1999). This motif defines an auxin-dependent expression pattern. We have previously shown that the expression of the *rolA* and *rolB* genes is inconsistent and IAA-dependent (Veremeichik et al. 2023b). The 30-day cultivation of pRiA4-transformed calli in the presence of IAA led to the induction of *rolA* gene

expression and immediate inhibition of *rolB* gene expression. Moreover, 30 days of cultivation of pRiA4-transformed calli on PGR-free media strongly reduced *rolA* gene expression and induced *rolB* gene expression. The presence or absence of IAA in the media had no effect on the expression of the *rolC* gene. However, we did not find information about the effect of auxins on the individual expression of the *rolA* gene. Thus, it can be assumed that a shift in biosynthesis in long-term cultured *rolA*-calli may be associated with changes in the hormonal status of the cell culture during long-term cultivation. Understanding these processes has encountered a number of difficulties. First, the homeostasis of hormones, especially auxins, in plant calli during long-term cultivation is unknown. Second, how IAA affects *rolA* expression is not known. Thus, to address this hypothesis, we first examined the effect of IAA on *rolA* gene expression. For this purpose, an additional cell culture of *R. cordifolia* was obtained and transformed with a new genetic construct carrying the *rolA* gene under the control of its own promoter. Using two independent cell cultures, we reliably showed that the expression of the *rolA* gene under the control of its own promoter is IAA dependent. In this context, determining how the hormonal status of a cell culture changes during long-term cultivation is necessary. However, this work requires scale and robust validation to identify general patterns, not just specific phenomena.

Interestingly, *rolA* gene expression led to a twofold increase in the AQ content in newly obtained calli. This result corresponds to that previously obtained. In 2008, it was shown that *rolA*-expressing calli of *R. cordifolia* RA, used in this work for long-term cultivation, contained twofold more AQ than did the control untransformed calli (Shkryl et al. 2008). After more than 5 years of continuous cultivation, a biosynthesis shift was observed (Veremeichik et al. 2019). In the present work, this activatory effect on *rolA* gene expression was confirmed after the next ten years of cultivation. Moreover, the composition of the AQ derivatives was more abundant in both of the analysed *rolA*-expressing calli lines than in the untransformed control culture. We propose a possible explanation for the *rolA*-mediated time-dependent activation of AQ biosynthesis. IAA dependence of *rolA* gene expression may determine the RolA-dependent modulation of IAA biosynthesis and metabolism. Moreover, the ability of *rolA*-expressing calli to grow on PGR-free media for a long period of time also indicates a possible role for RolA in the regulation of IAA biosynthesis. Whereas IAA and AQs are derivatives of the common precursor chorismate (Mano and Nemoto 2012; Bajguz and Piotrowska-Nic 2023), it can be hypothesised that RolA can affect the shikimic acid pathway. However, this assumption requires careful study and confirmation but also points to a new direction in the study of the function of the *rolA* gene.

However, the obtained data led to unexpected results. Identification of the IAA dependence of *rolA* gene expression made it possible to identify a new function of RolA. We showed that the expression of *rolA* leads to a strong decrease in intracellular ROS due to a decrease in the expression of ROS-generating genes, which in turn provokes a decrease in the expression of ROS detoxification genes. The data obtained are consistent with the previously obtained results and allow us to form a more complete picture of *rol*-mediated regulation of ROS metabolism in plant cells. In our previous study, to clarify the roles of *rolA* genes in PGR-dependent growth alterations, we analysed the dependence of *R. cordifolia* on ROS metabolism and IAA-mediated *rol* gene expression in wild pRiA4-transformed calli. The absence of PGR in the medium led to the inhibition of *rolA* gene expression accompanied by a high expression level of the *rolB* gene. The addition of media supplemented with IAA had the opposite effect: a decrease in ROS in the presence of IAA and an increase in its absence (Veremeichik et al. 2023b). In the present work, we showed that the expression of the *rolA* gene is IAA dependent and that the IAA-mediated increase in *rolA* gene expression led to a decrease in the expression of

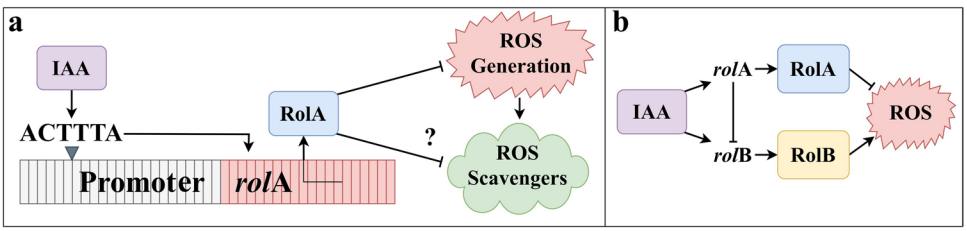

Fig. 6 A simplified model suggesting the possible auxin-dependent mechanism of the *rolA*-mediated action of the *rolB* gene. **a** The scheme shows that the promoter (gray block) of the *rol*A gene can be auxin regulated, as shown in the present study, due to the presence of the ACCTTTA motif for the auxin-dependent Dof protein (Baumann et al. 1999). IAA induces the expression of the *rolA* gene, which is accompanied by a decrease in the expression of genes encoding enzymes of the ROS metabolism system. **b** It can be assumed that the expression of the *rolA* gene blocks the expression of the *rolB* gene at the transcription level (Durand-Tardif et al. 1985), whereas the RolA protein, in addition, mitigates the RolB-induced activation of ROS signalling (Veremeichik et al. 2016) to prevent *rolB*-mediated growth inhibition

genes involved in ROS metabolism (Fig. 6a). The results obtained can be summarised in a diagram (Fig. 6b). When *rolA* genes are coexpressed, IAA-dependent expression of the *rolA* gene blocks the expression of the *rolB* gene (Tepfer 1984; Durand-Tardif et al. 1985; Capone et al. 1989), and there seems to be a mechanism preventing *rolA* and *rolB* from coexpressing. Furthermore, compared with the *rolB* and *rolC* promoters, the *rolA* promoter is more active (Schmülling et al. 1989). We showed that IAA-dependent expression of the *rolA* gene led to a decrease in ROS metabolism, as did the expression of *rolA* alone and in combination with other *rol* genes. The antagonistic interaction between *rolA* and *rolB* may prevent strong *rolB*-induced auxin sensitivity (Maurel et al. 1991) and oxidative bursts to balance the cell state (Fig. 6b). The biological roles of the *rol* genes are complementary. Each of them appears to have a distinct effect on host activities that are involved in determining root differentiation, according to Spena et al. (1987). The iRNA machinery can also control *rolA* and *rolB* gene expression. The core and accessory proteins of the microRNA processing apparatus (DCL1, AGO1, and AGO4) are encoded by genes whose expression is regulated by rolB (Bulgakov et al. 2015). Subsequent investigations of small RNAs derived from the T-DNA of *R. rhizogenes* in the hairy roots of *P. vulgaris* revealed that *rolA* is a dominant source of small RNAs, whereas no ArT-sRNAs are derived from the *rolC* gene (Pelaez et al. 2017). Moreover, MiR393 is absent in hairy roots but present in pRi-transformed calli. According to Pelaez et al. (2017), miR393 is believed to target major auxin receptors and may be important for development.

Recent research has demonstrated potential auxin-dependent contradiction between *rolA* and *rolB*, as well as potential targets and physiological consequences, such as ROS metabolism. The data we obtained and presented in this work need to be verified via a whole plant. Such studies will be especially interesting from an evolutionary perspective. Durable investigations of *rolA*-transformed cell cultures have made it possible to identify the function of RolA in the modulation of auxin homeostasis and secondary metabolism during long-term cultivation. The evolutionary role of the *rolA* gene as a possible modulator of auxin homeostasis can be determined by studying whole plants. First, it is necessary to clarify the effect of RolA on ROS metabolism in whole plants; second, it is necessary to determine the impact of the overexpression of the *rolA* gene on dynamic IAA homeostasis and, conversely, the influence of the dynamic homeostasis of auxins on *rolA* gene expression.

Supplementary Information The online version contains supplementary material available at https://doi.org/10.1007/s00425-024-04597-7.

Acknowledgements We thank researchers who have devoted their time and energy to the study of the structure and function of the *rol* genes. The analyses described in this work were performed using equipment from the Instrumental Centre for Biotechnology and Gene Engineering at the Federal Scientific Centre of East Asia Terrestrial Biodiversity of the Far East Branch of the Russian Academy of Sciences.

Author contributions GNV Conceptualization, Data curation, Project administration, Supervision, Validation, Visualization, Writing—original draft. VPB, DVB Resources, Funding acquisition. GNV, TOG, AAK, TYG, VPG, EVB, Investigation, Methodology, Formal Analysis.

Funding Financial support was provided by the Russian Science Foundation, Grant no. 23–24-00215 (Bulgakov D.V.).

Data availability The datasets generated during and/or analysed during the current study are available from the corresponding author upon reasonable request. Code availability Not applicable.

Declarations

Conflict of interest The authors declare that they have no competing interests.

Ethics approval Not applicable.

Consent to participate Not applicable.

Consent for publication All the authors whose names appeared on the submission approved the version to be published and agreed to be accountable for all aspects of the work in ensuring that the questions related to the accuracy or integrity of any part of the work were appropriately investigated and resolved.

References

Altschul SF, Gish W, Miller W, Myers EW, Lipman DJ (1990) Basic local alignment search tool. J Mol Biol 215(3):403–410. https://doi.org/10.1016/S0022-2836(05)80360-2

Amanullah M, Mirza B, Zia M (2016) Production of artemisinin and its derivatives in hairy roots of *Artemisia dubia* induced by *rol*A gene transformation. Pak J Bot 48:699–706

Aubin E, El Baidouri M, Panaud O (2021) Horizontal gene transfers in plants. Life 11:857. https://doi.org/10.3390/life11080857

Bajguz A, Piotrowska-Niczyporuk A (2023) Biosynthetic pathways of hormones in plants. Metabolites 13(8):884. https://doi.org/10.3390/metabo13080884

Barros LM, Curtis R, Viana AA, Campos L, Carneiro M (2003) Fused RolA protein enhances β-glucoronidase activity 50-fold: implication for RolA mechanism of action. Protein Pept Lett 10:303–311. https://doi.org/10.2174/0929866033478951

Baumann K, De Paolis A, Costantino P, Gualberti G (1999) The DNA binding site of the Dof protein NtBBF1 is essential for tissue-specific and auxin-regulated expression of the rolB oncogene in plants. Plant Cell 11(3):323–334. https://doi.org/10.1105/tpc.11.3.323

Bettini PP, Santangelo E, Baraldi R, Rapparini F, Mosconi P, Crinò P, Mauro ML (2016) *Agrobacterium rhizogenes rol*A gene promotes tolerance to *Fusarium oxysporum* f. sp. *lycopersici* in transgenic tomato plants (*Solanum lycopersicum* L.). J Plant Biochem Biotechnol 25:225–233. https://doi.org/10.1007/s13562-015-0328-4

Boldizsár I, Szucs Z, Füzfai Z, Molnár-Perl I (2006) Identification and quantification of the constituents of madder root by gas

chromatography and high-performance liquid chromatography. J Chromatogr A 1133(1–2):259–274. https://doi.org/10.1016/j.chroma.2006.08.021

Bulgakov VP, Tchernoded GK, Mischenko NP, Khodakovskaya MV, Glazunov VP, Radchenko SV, Zvereva EV, Fedoreyev SA, Zhuravlev YN (2002) Effect of salicylic acid, methyl jasmonate, ethephon and cantharidin on anthraquinone production by *Rubia cordifolia* callus cultures transformed with the *rolB* and *rolC* genes. J Biotechnol 97(3):213–221. https://doi.org/10.1016/s0168-1656(02)00067-6

Bulgakov VP, Aminin DL, Shkryl YN, Gorpenchenko TY, Veremeichik GN, Dmitrenok PS, Zhuravlev YN (2008) Suppression of reactive oxygen species and enhanced stress tolerance in *Rubia cordifolia* cells expressing the *rol*C oncogene. Mol Plant Microbe Interact 21(12):1561–1570. https://doi.org/10.1094/mpmi-21-12-1561

Bulgakov VP, Shkryl YN, Veremeichik GN, Gorpenchenko TY, Vereshchagina YV (2011) Application of Agrobacterium *rol* genes in plant biotechnology: a natural phenomenon of secondary metabolism regulation. INTECH. https://doi.org/10.5772/24200

Bulgakov VP, Gorpenchenko TY, Veremeichik GN, Shkryl YN, Tchernoded GK, Bulgakov DV, Aminin DL, Zhuravlev YN (2012) The *rolB* gene suppresses reactive oxygen species in transformed plant cells through the sustained activation of antioxidant defense. Plant Physiol 158(3):1371–1381. https://doi.org/10.1104/pp.111.191494

Bulgakov VP, Shkryl YN, Veremeichik GN, Gorpenchenko TY, Vereshchagina YV (2013) Recent advances in the understanding of *Agrobacterium rhizogenes*-derived genes and their effects on stress resistance and plant metabolism. Adv Biochem Eng Biotechnol 134:1–22. https://doi.org/10.1007/10_2013_179

Bulgakov VP, Veremeichik GN, Shkryl YN (2015) The *rolB* gene activates the expression of genes encoding microRNA processing machinery. Biotechnol Lett 37(4):921–925. https://doi.org/10.1007/s10529-014-1743-7

Capone I, Spanò L, Cardarelli M, Bellincampi D, Petit A, Costantino P (1989) Induction and growth properties of carrot roots with different complements of *Agrobacterium rhizogenes* T-DNA. Plant Mol Biol 13:43–52. https://doi.org/10.1007/BF00027334

Chabi Sika K, Kefela T, Adoukonou-Sagbadja H, Ahoton L, Saidou A, Baba-Moussa S, Baptiste L, Kotchoni L, Gachomo S, Emma W (2015) A simple and efficient genomic DNA extraction protocol for large scale genetic analyses of plant biological systems. Plant Gene 1:43–45. https://doi.org/10.1016/j.plgene.2015.03.001

Chen K, Zhurbenko P, Danilov L, Matveeva T, Otten L (2022) Conservation of an *Agrobacterium* cTDNA insert in *Camellia* section Thea reveals the ancient origin of tea plants from a genetically modified ancestor. Front Plant Sci 13:997762. https://doi.org/10.3389/fpls.2022.997762

Dehio C, Grossmann K, Schell J, Schmülling T (1993) Phenotype and hormonal status of transgenic tobacco plants overexpressing the *rolA* gene of *Agrobacterium rhizogenes* T-DNA. Plant Mol Biol 23:1199–1210. https://doi.org/10.1007/BF00042353

Derksen GC, Niederländer HA, van Beek TA (2002) Analysis of anthraquinones in Rubia tinctorum L. by liquid chromatography coupled with diode-array UV and mass spectrometric detection. J Chromatogr A 978(1–2):119–127. https://doi.org/10.1016/s0021-9673(02)01412-7

Desmet S, Dhooghe E, De Keyser E, Van Huylenbroeck J, Müller R, Geelen D, Lütken H (2020a) Rhizogenic agrobacteria as an innovative tool for plant breeding: current achievements and limitations. Appl Microbiol Biotechnol 104:2435–2451. https://doi.org/10.1007/s00253-020-10403-7

Desmet S, Dhooghe E, De Keyser E, Quataert P, Eeckhaut T, Van Huylenbroeck J, Geelen D (2020b) Segregation of *rol* genes in two generations of *Sinningia speciosa* engineered through wild type *Rhizobium rhizogenes*. Front Plant Sci 11:859. https://doi.org/10.3389/fpls.2020.00859

Desmet S, Dhooghe E, De Keyser E, Van Huylenbroeck J, Geelen D (2021) Compact shoot architecture of *Osteospermum fruticosum* transformed with *Rhizobium rhizogenes*. Plant Cell Rep 40:1665–1678. https://doi.org/10.1007/s00299-021-02719-z

Durand-Tardif M, Broglie R, Slightom J, Tepfer D (1985) Structure and expression of Ri T-DNA from *Agrobacterium rhizogenes* in *Nicotiana tabacum*. J Mol Biol 186:557–564. https://doi.org/10.1016/0022-2836(85)90130-5

Guo M, Ye J, Gao D, Xu N, Yang J (2019) *Agrobacterium*-mediated horizontal gene transfer: mechanism, biotechnological application, potential risk and forestalling strategy. Biotechnol Adv 37:259–270. https://doi.org/10.1016/j.biotechadv.2018.12.008

Gutierrez-Valdes N, Häkkinen ST, Lemasson C, Guillet M, Oksman-Caldentey K-M, Ritala A, Cardon F (2020) Hairy root cultures—a versatile tool with multiple applications. Front Plant Sci 11:33. https://doi.org/10.3389/fpls.2020.00033

Hayashi K, Hashimoto N, Daigen M, Ashikawa I (2004) Development of PCR-based SNP markers for rice blast resistance genes at the *Piz* locus. Theor Appl Genet 108(7):1212–1220. https://doi.org/10.1007/s00122-003-1553-0

Holefors A, Xue Z-T, Welander M (1998) Transformation of the apple rootstock M26 with the *rolA* gene and its influence on growth. Plant Sci 136:69–78. https://doi.org/10.1016/S0168-9452(98)00106-X

Hood EE, Gelvin SB, Melchers LS, Hoekema A (1993) New *Agrobacterium* helper plasmids for gene transfer to plants. Transgenic Res 2(4):208–218. https://doi.org/10.1007/BF01977351

Hooykaas MJG, Hooykaas PJJ (2021) The genome sequence of hairy root *Rhizobium rhizogenes* strain LBA9402: Bioinformatics analysis suggests the presence of a new opine system in the agropine Ri plasmid. Microbiol Open 10(2):e1180. https://doi.org/10.1002/mbo3.1180

Magrelli A, Langenkemper K, Dehio C, Schell J, Spena A (1994) Splicing of the *rolA* transcript of *Agrobacterium rhizogenes* in *Arabidopsis*. Science 266:1986–1988. https://doi.org/10.1126/science.7528444

Mano Y, Nemoto K (2012) The pathway of auxin biosynthesis in plants. J Exp Bot 63(8):2853–2872. https://doi.org/10.1093/jxb/ers091

Matveeva T, Otten L (2019) Widespread occurrence of natural genetic transformation of plants by *Agrobacterium*. Plant Mol Biol 101:415–437. https://doi.org/10.1007/s11103-019-00913-y

Matveeva T, Otten L (2021) Opine biosynthesis in naturally transgenic plants: Genes and products. Phytochemistry 189:112813. https://doi.org/10.1016/j.phytochem.2021.112813

Maurel C, Barbier-Brygoo H, Spena A, Tempé J, Guern J (1991) Single *rol* genes from the *Agrobacterium rhizogenes* T_L-DNA alter some of the cellular responses to auxin in *Nicotiana tabacum*. Plant Physiol 97:212–216. https://doi.org/10.1104/pp.97.1.212

Mischenko NP, Fedoreyev SA, Glazunov VP, Chernoded GK, Bulgakov VP, Zhuravlev YN (1999) Anthraquinone production by callus cultures of *Rubia cordifolia*. Fitoterapia 70:552–557. https://doi.org/10.1016/S0367-326X(99)00085-4

Mittler R (2017) ROS are good. Trends Plant Sci 22(1):11–19. https://doi.org/10.1016/j.tplants.2016.08.002

Otten L (2018) How *Agrobacterium*, a natural genetic engineer, became a tool for modern agriculture. Adv Bot Res 86:17–44. https://doi.org/10.1016/bs.abr.2017.11.002

Palazon J, Cusido RM, Roig C, Pinol MT (1997) Effect of *rol* genes from *Agrobacterium rhizogenes* TL-DNA on nicotine production in tobacco root cultures. Plant Physiol Biochem 35:155–162

Pandolfini T, Storlazzi A, Calabria E, Defez R, Spena A (2000) The spliceosomal intron of the *rolA* gene of *Agrobacterium*

rhizogenes is a prokaryotic promoter. Mol Microbiol 35:1326–1334. https://doi.org/10.1046/j.1365-2958.2000.01810.x

Pelaez P, Hernandez-Lopez A, Estrada-Navarrete G, Sanchez F (2017) Small RNAs derived from the T-DNA of *Agrobacterium rhizogenes* in hairy roots of *Phaseolus vulgaris*. Front Plant Sci 8:96. https://doi.org/10.3389/fpls.2017.00096

Philips JG, Martin-Avila E, Robold AV (2022) Horizontal gene transfer from genetically modified plants – regulatory considerations. Front Bioeng Biotechnol 10:971402. https://doi.org/10.3389/fbioe.2022

Pujari I, Babu VS (2022) *Rhizobium rhizogenes* infection in threatened Indian orchid *Dendrobium ovatum* mobilises 'Moscatilin' to enhance plant defenses. 3Biotech 12:119. https://doi.org/10.1007/s13205-022-03180-9

Rigden DJ, Carneiro M (1999) A structural model for the RolA protein and its interaction with DNA. Proteins 37:697–708. https://doi.org/10.1002/(sici)1097-0134(19991201)37:4%3c697::aid-prot18%3e3.0.co;2-y

Sambrook J, Fritsch ER, Maniatis T (1989) Molecular cloning: A laboratory manual, 2nd edn. Cold Spring Harbor Laboratory Press, Cold Spring Harbor, NY

Sarkar S, Ghosh I, Roychowdhury D, Jha S (2018). In: Kumar N (ed) Biotechnological approaches for medicinal and aromatic plants. Springer, Singapore, pp 27–51. https://doi.org/10.1007/978-981-13-0535-1_2

Schmülling T, Schell J, Spena A (1989) Promoters of the *rolA*, *B*, and *C* genes of *Agrobacterium rhizogenes* are differentially regulated in transgenic plants. Plant Cell 1:665–670. https://doi.org/10.1105/tpc.1.7.665

Serino G, Clerot D, Brevet J, Costantino P, Cardarelli M (1994) *rol* genes of *Agrobacterium rhizogenes* cucumopine strain: sequence, effects and pattern of expression. Plant Mol Biol 26:415–422. https://doi.org/10.1007/BF00039550

Shkryl YN, Veremeichik GN, Bulgakov VP, Tchernoded GK, Mischenko NP, Fedoreyev SA, Zhuravlev YN (2008) Individual and combined effects of the *rol* A, B, and C genes on anthraquinone production in *Rubia cordifolia* transformed calli. Biotechnol Bioeng 100:118–125. https://doi.org/10.1002/bit.21727

Shkryl YN, Veremeichik GN, Bulgakov VP, Gorpenchenko TY, Aminin DL, Zhuravlev YN (2010) Decreased ROS level and activation of antioxidant gene expression in *Agrobacterium rhizogenes* pRiA4-transformed calli of *Rubia cordifolia*. Planta 232:1023–1032. https://doi.org/10.1007/s00425-010-1237-3

Shkryl YN, Veremeichik GN, Bulgakov VP, Zhuravlev YN (2011) Induction of anthraquinone biosynthesis in *Rubia cordifolia* cells by heterologous expression of a calcium-dependent protein kinase gene. Biotechnol Bioeng 108:1734–1738. https://doi.org/10.1002/bit.23077

Shkryl YN, Veremeichik GN, Makhazen DS, Silantieva SA, Mishchenko NP, Vasileva ES, Fedoreyev SA, Bulgakov VP (2016) Increase of anthraquinone content in *Rubia cordifolia* cells transformed by native and constitutively active forms of the *AtCPK1* gene. Plant Cell Rep 9(35):19017–21916. https://doi.org/10.1007/s00299-016-2005-z

Shkryl YN, Veremeichik GN, Avramenko TV, Gorpenchenko TY, Tchernoded GK, Bulgakov VP (2022) Transcriptional regulation of enzymes involved in ROS metabolism and abiotic stress resistance in *rol*C-transformed cell cultures. Plant Growth Regul 97:485–497. https://doi.org/10.1007/s10725-022-00812-1

Sinkar VP, Pythoud F, White FF, Nester EW, Gordon MP (1988) *rol*A locus of the Ri plasmid directs developmental abnormalities in transgenic tobacco plants. Genes Dev 2:688–697. https://doi.org/10.1101/gad.2.6.688

Smytch SJ, McHughen A, Kershen EJD, Ramage C, Parrott W (2021) Removing politics from innovations that improve food security. Transgenic Res 30:601–612. https://doi.org/10.1007/s11248-021-00261-y

Spena A, Langenkemper K (1997) Mutational analysis of the *rolA* gene of *Agrobacterium rhizogenes* in tobacco: function of the *rolA* pre-mRNA intron and RolA proteins defective in their biological activity. Genet Res 69:11–15. https://doi.org/10.1017/s0016672396002534

Spena A, Schmülling T, Koncz C, Schell JS (1987) Independent and synergistic activity of *rolA*, *B*, and *C* loci in stimulating abnormal growth in plants. EMBO J 6:3891–3899. https://doi.org/10.1002/j.1460-2075.1987.tb02729.x

Stavnstrup S, Molina J, Lütken H, Müller R, Hegelund J (2020) Ancient horizontal gene transfer from *Rhizobium rhizogenes* to European genera of the Figwort family (Scrophulariaceae). Euphytica 216:186. https://doi.org/10.1007/s10681-020-02722-7

Tepfer D (1984) Transformation of several species of higher plants by *Agrobacterium rhizogenes*: sexual transmission of the transformed genotype and phenotype. Cell 37:959–967. https://doi.org/10.1016/0092-8674(84)90430-6

Tripathi YB, Sharma M, Manickam M (1997) Rubiadin, a new antioxidant from *Rubia cordifolia*. Indian J Biochem Biophys 34(3):302–306

Tzfira T, Tian GW, Lacroix B, Vyas S, Li J, Leitner-Dagan Y, Krichevsky A, Taylor T, Vainstein A, Citovsky V (2005) pSAT vectors: a modular series of plasmids for autofluorescent protein tagging and expression of multiple genes in plants. Plant Mol Biol 57(4):503–516. https://doi.org/10.1007/s11103-005-0340-5

Veremeichik GN, Bulgakov VP, Shkryl YN (2016) Modulation of NADPH-oxidase gene expression in *rol*B-transformed calli of *Arabidopsis thaliana* and *Rubia cordifolia*. Plant Physiol Biochem 105:282–289. https://doi.org/10.1016/j.plaphy.2016.05.014

Veremeichik GN, Bulgakov VP, Shkryl YN, Silantieva SA, Makhazen DS, Tchernoded GK, Mischenko NP, Fedoreyev SA, Vasileva EA (2019) Activation of anthraquinone biosynthesis in long-cultured callus culture of *Rubia cordifolia* transformed with the *rol*A plant oncogene. J Biotechnol 306:38–46. https://doi.org/10.1016/j.jbiotec.2019.09.007

Veremeichik GN, Shkry YN, Gorpenchenko TY, Silantieva SA, Avramenko TV, Brodovskaya EV, Bulgakov VP (2021) Inactivation of the auto-inhibitory domain in *Arabidopsis AtCPK1* leads to increased salt, cold and heat tolerance in the *AtCPK1*-transformed *Rubia cordifolia* L cell cultures. Plant Physiol Biochem 159:372–382. https://doi.org/10.1016/j.plaphy.2020.12.031

Veremeichik GN, Shkryl YN, Rusapetova TV, Silantieva SA, Grigorchuk VP, Velansky PV, Brodovskaya EV, Konnova YA, Khopta AA, Bulgakov DV, Bulgakov VP (2022) Overexpression of the A4-*rol*B gene from the pRiA4 of *Rhizobium rhizogenes* modulates hormones homeostasis and leads to an increase of flavonoid accumulation and drought tolerance in *Arabidopsis thaliana* transgenic plants. Planta 256:8. https://doi.org/10.1007/s00425-022-03927-x

Veremeichik GN, Bulgakov DV, Solomatina TO, Makhazen DS (2023a) In the interkingdom horizontal gene transfer, the small *rol*A gene is a big mystery. Appl Microbiol Biotechnol 107(7–8):2097–2109. https://doi.org/10.1007/s00253-023-12454-y

Veremeichik GN, Gorpenchenko TY, Rusapetova TV, Brodovskaya EV, Tchernoded GK, Bulgakov DV, Shkryl YN, Bulgakov VP (2023) Auxin-dependent regulation of growth via rolB-induced modulation of the ROS metabolism in the long-term cultivated pRiA4-transformed Rubia cordifolia L. calli. Plant Physiol Biochem 202:107932. https://doi.org/10.1016/j.plaphy.2023.107932

Vereshchagina YV, Bulgakov VP, Grigorchuk VP, Rybin VG, Veremeichik GN, Tchernoded GK, Gorpenchenko TY, Koren OG, Phan NH, Minh NT, Chau LT, Zhuravlev YN (2014) The *rol*C gene increases caffeoylquinic acid production in transformed artichoke cells. Appl Microbiol Biotechnol 98(18):7773–7780. https://doi.org/10.1007/s00253-014-5869-2

White FF, Ghidossi G, Gordon MP, Nester EW (1982) Tumor induction by *Agrobacterium rhizogenes* involves the transfer of plasmid DNA to the plant genome. Proc Nat Acad Sci USA 79:3193–3197. https://doi.org/10.1073/pnas.79.10.3193

Xue Z-T, Holefors A, Welander M (2008) Intron splicing in 5′ untranslated region of the *rolA* transcript in transgenic apple. J Plant Physiol 165:544–552. https://doi.org/10.1016/j.jplph.2006.11.010

Zhu L-H, Ahlman A, Li X-Y, Welander M (2001) Integration of the *rol*A gene into the genome of the vigorous apple rootstock A2 reduced plant height and shortened internodes. J Hortic Sci Biotechnol 76:758–763. https://doi.org/10.1080/14620316.2001.11511442

Zia M, Mirza B, Malik SA, Chaudhary MF (2010) Expression of *rol* genes in transgenic soybean (*Glycine max* L.) leads to changes in plant phenotype, leaf morphology, and flowering time. Plant Cell Tiss Organ Cult 103:227–236. https://doi.org/10.1007/s11240-010-9771-z